

POPULATIONS OF HIGH-LUMINOSITY DENSITY-BOUNDED H II REGIONS IN SPIRAL GALAXIES: EVIDENCE AND IMPLICATIONS

J. E. BECKMAN,^{1,2} M. ROZAS,¹ A. ZURITA,¹ R. A. WATSON,¹ AND J. H. KNAPEN^{3,4}

Received 1998 November 9; accepted 2000 March 8

ABSTRACT

We present evidence that the H II regions of high luminosity in disk galaxies may be density bounded, so that a significant fraction of the ionizing photons emitted by their exciting OB stars escapes from the regions. The key piece of evidence is the presence of glitches, local sharp peaks at an apparently invariant luminosity, in the H α luminosity functions of the populations of H II regions. The apparently invariant luminosity is defined as the Strömgen luminosity (L_{Str}), such that $L_{\text{H}\alpha} = L_{\text{Str}} = 10^{38.6} \pm 10^{0.1}$ ergs s⁻¹ (no other peaks are found in any of the luminosity functions) accompanying a steepening of slope for $L_{\text{H}\alpha} > L_{\text{Str}}$. This behavior is readily explicable by a physical model in which (1) the transition at $L_{\text{H}\alpha} = L_{\text{Str}}$ marks a change from essentially ionization bounding at low luminosities to density bounding at higher values and (2) for this to occur the law relating stellar mass in massive star-forming clouds to the mass of the placental cloud must be such that the ionizing photon flux produced within the cloud is a function that rises more steeply than the mass of the cloud. Supporting evidence for the hypothesis of this transition is also presented: measurements of the central surface brightnesses of H II regions for $L_{\text{H}\alpha} < L_{\text{Str}}$ are proportional to $L_{\text{H}\alpha}^{1/3}$, as expected for ionization bounding, but show a sharp trend to a steeper dependence for $L_{\text{H}\alpha} > L_{\text{Str}}$, and the observed relation between the internal turbulence velocity parameter, σ , and the luminosity, L , at high luminosities can be well explained if these regions are density bounded. If confirmed, the density-bounding hypothesis would have a number of interesting implications. It would imply that the density-bounded regions were the main sources of the photons that ionize the diffuse gas in disk galaxies. Our estimates, based on the hypothesis, indicate that these regions emit sufficient Lyman continuum photons not only to ionize the diffuse medium but to cause a typical spiral to emit significant ionizing flux into the intergalactic medium. The low scatter observed in L_{Str} , less than 0.1 mag rms in the still quite small sample measured to date, is an invitation to widen the database and to calibrate against primary standards to obtain a precise ($\sim 10^5 L_{\odot}$) widely distributed standard candle.

Key words: galaxies: individual (NGC 157, NGC 3359, NGC 6814, NGC 7479) —
galaxies: spiral — H II regions

1. INTRODUCTION

The basic theory for modeling a gaseous region around a hot star was first given by Zanstra (1931) for planetary nebulae and applied to H II regions by Strömgen (1939), who quantified the relation between the radius of the ionized zone and the temperature and luminosity of the central exciting star. He showed that in a uniform medium the transition layer between fully ionized and neutral gas, a structure since termed a “Strömgen sphere,” will be thin compared with the radius. This will occur in a large placental neutral cloud of sufficient dimension to absorb all the ionizing photons (those in the Lyman continuum in the case of atomic hydrogen), in which case the H II region is “ionization bounded.” The case in which the cloud is not large enough to absorb all the ionizing radiation was first dealt with by Hummer & Seaton (1964) for planetary nebulae, which are then termed “optically thin.” An H II region formed in these circumstances, where the cloud radius is less than that of the Strömgen sphere, is termed “density bounded” or “matter bounded.”

There is ample evidence that H II regions are not homogeneous in density. Measurements of local electron densities using line ratios are typically 2 orders of magnitude higher than mean electron densities estimated using diametral emission measures (for a clear recent example, see Rozas, Knapen, & Beckman 1996b), explicable if a region comprises knots of high density embedded in a lower density plasma. The fractional volume dense enough to contribute measurably in emission lines such as H α has been termed the “filling factor” (e.g., Osterbrock 1989). An H II region with this structure will form a Strömgen sphere provided that the local density variations are on scales that are small compared with the H II region diameter and that the mean density varies little on the scale of the diameter. This condition appears to hold well for regions over a wide range of H α luminosities, up to a critical value, which we will be able to quantify from observations as described below. The regions in this range are ionization bounded. At higher luminosities our evidence, which will be described in this paper, points toward an increasing tendency for the photon output from the ionizing stars to overflow the cloud in which they have formed.

One type of evidence comes from the measurements of a change in slope of the luminosity function in H α of complete populations of H II regions in the set of nearby spirals. Previous detections of this change have been reported in the literature, notably in earlier work by Hodge (1987), Kennicutt (1984), Kennicutt, Edgar, & Hodge (1989), and most

¹ Instituto de Astrofísica de Canarias, Calle Vía Láctea, E-38200 La Laguna, Tenerife, Spain.

² Consejo Superior de Investigaciones Científicas, CSIC, Spain.

³ University of Hertfordshire, Department of Physical Sciences, College Lane, Hatfield, Hertfordshire AL10 9AB, UK.

⁴ Isaac Newton Group of Telescopes, Apdo. de Correos 321, E-38780 Santa Cruz de La Palma, Spain.

recently by McCall, Straker, & Uomoto (1996) and Kingsburgh & McCall (1998), as well as ourselves (Rozas, Beckman, & Knapen 1996a). It is interesting to note, however, that the change in slope varies little from object to object. We will elaborate this point during the development of the present paper.

Statistical studies of the relation between the H α luminosities, $L_{\text{H}\alpha}$, of complete samples of H II regions in nearby large spirals and their volumes (Cepa & Beckman 1989, 1990; Knapen et al. 1993; Rozas et al. 1996a) show that to a first approximation these are proportional. Taken as a complete description of the observations, this would imply, at least statistically, two properties: (1) the H II regions obey a single physical regime, which should be that of ionization bounding, and (2) the densities of the clouds in which the H II regions are formed differ little from cloud to cloud within a galaxy and from galaxy to galaxy. We will see that at very high luminosities, departures from this first-order behavior are dominant. Illustrations of these points may be found in a number of articles in the literature, where the H α luminosities of individually measured H II regions have been plotted logarithmically versus the cubes of their radii (Cepa & Beckman 1989, 1990; Knapen et al. 1993; Rozas et al. 1996b, 1999). In these articles, it is shown that for eight galaxies there is a close to linear relation between the H α luminosity and the volume of the H II regions in the range $37.5 < \log L_{\text{H}\alpha} < 39.5$, as pointed out by Cepa & Beckman (1990). This implies that the product of the filling factor, the electron density, and the ionized hydrogen density does not change very much over this range, although in all the galaxies there is a clear tendency for it to increase at the highest luminosities.

It is not entirely ruled out that the filling factor and mean density might vary independently with a relation that leaves their product invariant, but this would amount to a ‘‘conspiracy,’’ and it is more reasonable to assume that none of the cited parameters vary strongly. The general picture is of H II regions as spongy structures that may indeed have fractal characteristics as suggested by Elmegreen (1997) but with a degree of clumping and an average density that do not depend strongly on luminosity. However, in all the plots of $\log L_{\text{H}\alpha}$ versus r^3 cited above, there is a significant trend to steeper gradients at higher luminosities, which means that here the densities and/or the filling factors of the regions must be increasing.

The evidence that we present below points to a rather sharp change in the properties of the H II regions occurring at an H α luminosity that appears to vary very little from galaxy to galaxy. We will show that one would in fact expect, on reasonable physical grounds, the most luminous regions to be producing more ionizing photons than can be absorbed in their placental clouds, whereas this should not be true globally for the less luminous regions. We can predict from a model in which there is a transition between ionization bounding at lower luminosities and density bounding at higher luminosities that there should be an accumulation of H II regions around the luminosity of the transition (which we have termed L_{Str} , i.e., the Strömgen transition) between the two regimes, and this accumulation is in fact found as a glitch in the H α luminosity function of the galaxies observed. It is by no means easy to reproduce these observations with alternative hypotheses. Two aspects of the density-bounding phenomenon would be of particular interest. Since the most luminous regions are those from which we predict the highest proportion of Lyman contin-

uum photons are escaping, these regions are candidates for the principal ionizing sources of the diffuse interstellar medium in large spirals and may contribute significantly to the intergalactic ionizing field. Also, the transition between ionization bounding and density bounding appears to take place over a narrow range in $L_{\text{H}\alpha}$, and while the sample of results presented here is not large, this point is worth following up because a high-luminosity feature of this kind would have its uses as a powerful, precise, and nontransient standard candle. However, the detailed interpretation of the surface brightness data is not obvious, and furthermore, spectroscopic observations will be important to follow up the arguments presented here.

In § 2, we present the evidence about the change in properties of the H II regions. In § 3, we present scaling relations that support the model of density bounding for the highest luminosity regions and a set of alternative models aimed at explaining the observed glitches in the luminosity functions of H II regions in the galaxies observed. In § 4, we discuss the implications of our models for the diffuse H α emission from the warm ionized medium. In § 5, we summarize our conclusions, outline the observations required to deepen our understanding of the transition phenomenon, and suggest applications to the correction of the global star formation rates in galaxies and to the measurement of intergalactic distances.

2. EVIDENCE FOR A CHANGE IN PHYSICAL REGIME

2.1. Luminosity Functions

In a set of published papers stretching back over the past decade, we have published luminosity functions (LFs) in H α for the H II regions in spiral galaxies, the majority of which were in absolutely calibrated fluxes (Cepa & Beckman 1989, 1990; Knapen et al. 1993; Rozas et al. 1996a). It was while inspecting these LFs and the LF from Rand (1992) that we found the feature that led us to postulate the transition from ionization bounding to density bounding. All the LFs showed an abrupt change in slope accompanied by a glitch: an upward jump in the value of the LF at a luminosity close to $\log L_{\text{H}\alpha} = 38.6$ ($L_{\text{H}\alpha}$ in ergs per second). In Figure 1 we show an improved analysis of the LFs originally given in Rozas et al. (1996b) for the galaxies NGC 157, 3631, 6764, and 6951, in Knapen et al. (1993) for NGC 6814, and in Rand (1992) for M51, in which the principal change has been an effective rebinning into bins of 0.1 dex in luminosity. The new treatment of the data uses a three-dimensional surface fit of $\log L_{\text{H}\alpha}$ against number count ($\log N$) and diameter, which in Figure 1 has been projected into the ($\log L_{\text{H}\alpha}$, $\log N$)-plane with a resolution of 0.1 dex. The data show an absence of peaks in each LF except for the peak at the transition luminosity which, as seen, is accompanied by a change in the slope of the LF to steeper values at luminosities higher than that of the transition.

We carried out a specific check on NGC 157 to see how the glitch peak is affected if, instead of using a limiting surface brightness contour to define the integrated brightness of each H II region, we applied a cutoff at a constant fraction of the peak luminosity. This technique (percentage of peak photometry PPF) was described by Kingsburgh & McCall (1996); it avoids problems of signal-to-noise ratios (S/Ns) at the boundaries of the H II regions and should be superior to the limiting surface brightness method (fixed threshold photometry, FTP) for sets of geometrically

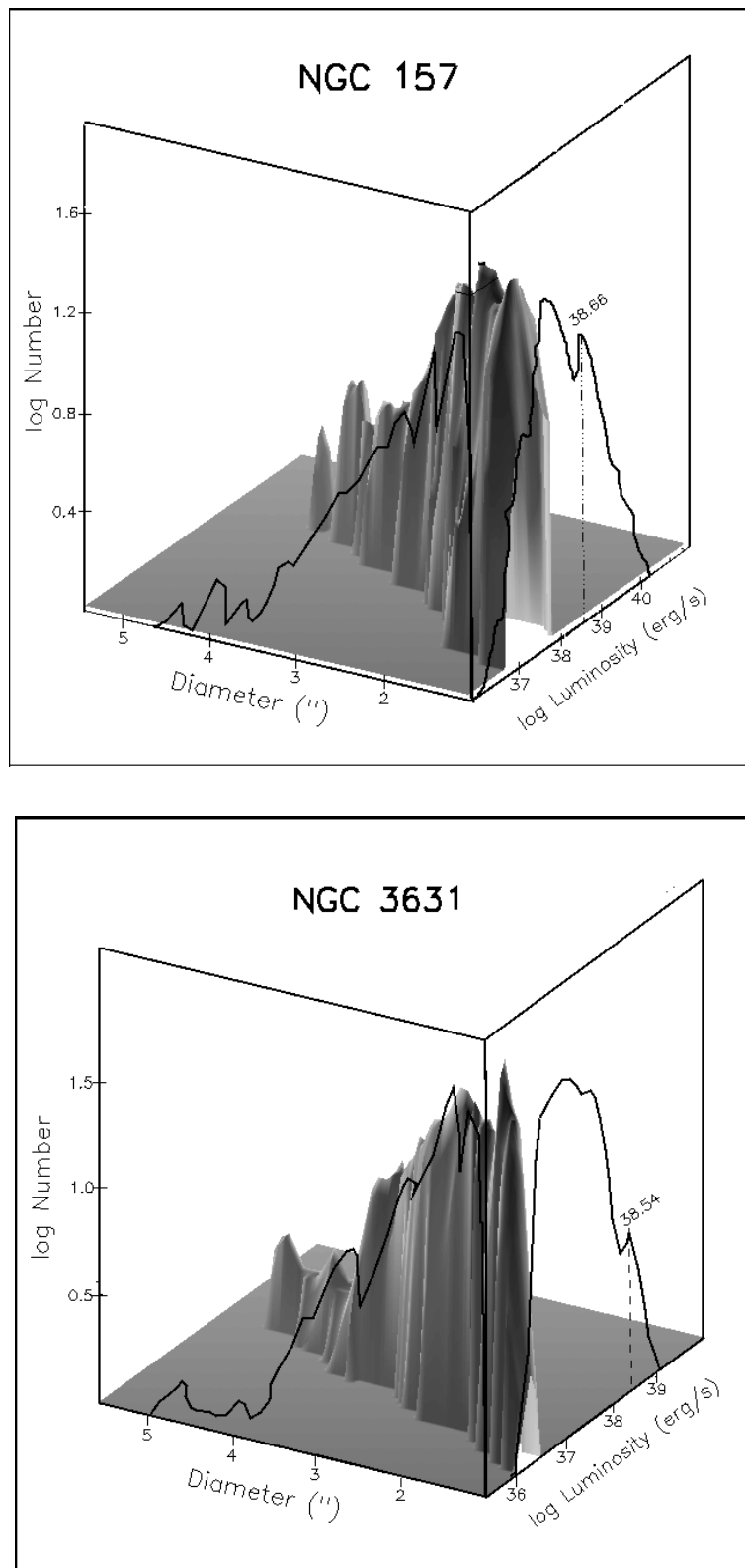


FIG. 1.—Three-dimensional surfaces: best fits to the observed data representing the numbers, N , diameters, d , and H α luminosities, $L_{\text{H}\alpha}$, of the H II regions in six galaxies. The projections in the $(\log N, \log L_{\text{H}\alpha})$ -plane are LFs with effective binning of 0.1 dex. The broad peaks and declines to low $L_{\text{H}\alpha}$ are caused by observational selection: low-luminosity regions are increasingly difficult to measure reliably below $\log L_{\text{H}\alpha} \sim 37$, though all samples are complete to below $\log L_{\text{H}\alpha} = 38$. The sharp peaks at $L_{\text{H}\alpha} \sim 38.6$ are presumably due to the transition from ionization bounding to density bounding (see text for details).

homologous regions. If there is a trend in varying the internal brightness gradient with luminosity, the PPF technique is liable to imprecision. In the present context, the most luminous regions have very bright centers and extended

halos, so that PPF tends to underestimate their luminosities. This was confirmed with the LF of NGC 157, which fell off more rapidly at high $L_{\text{H}\alpha}$ with PPF than with our normal technique, i.e., FTP. In spite of this, the glitch

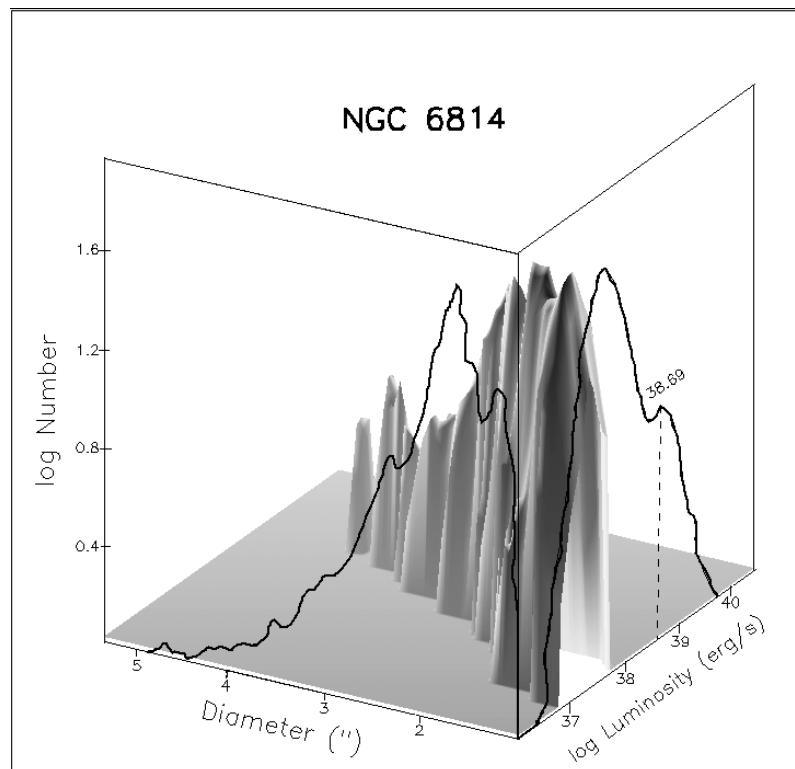
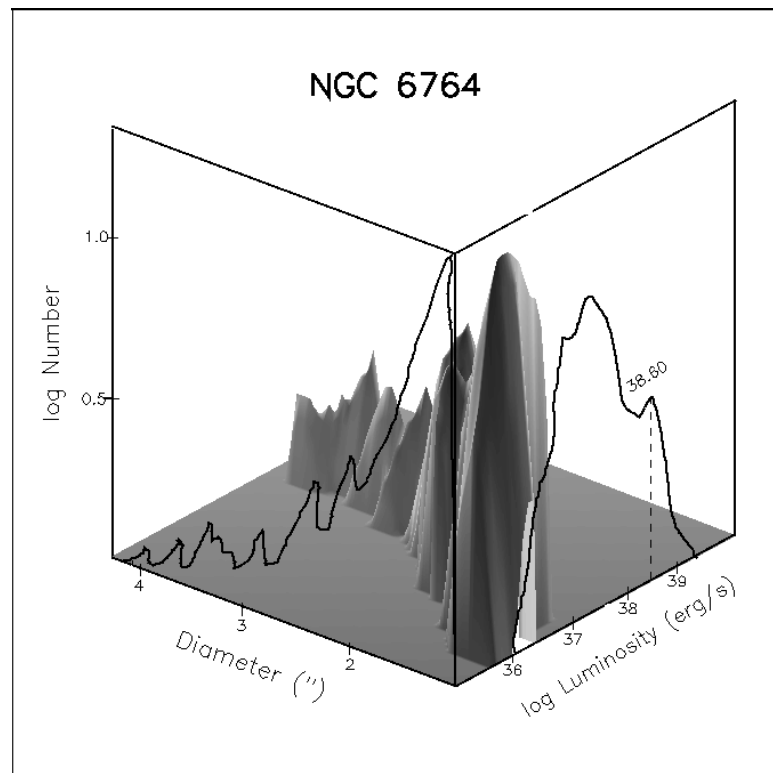


FIG. 1.—Continued

showed up at the same luminosity but at a statistically less significant level because fewer H II regions were involved.

To check that a peak is plausibly due to a truly collective property of the H II regions and is not merely a statistical fluctuation, we took the mean value, $N(m)$, of the number of H II regions in the bins to either side of the peak,

subtracted this from the value $N(\text{max})$ of the number of regions at the peak, and computed $[N(\text{max}) - N(m)] / [N(\text{max})]^{1/2}$. Values between 1 and 2 were found for each of the galaxies, with a mean of 1.7. Thus, the individual peaks are just significant, but if we were looking at a single galaxy and had no other kinds of observational evidence we

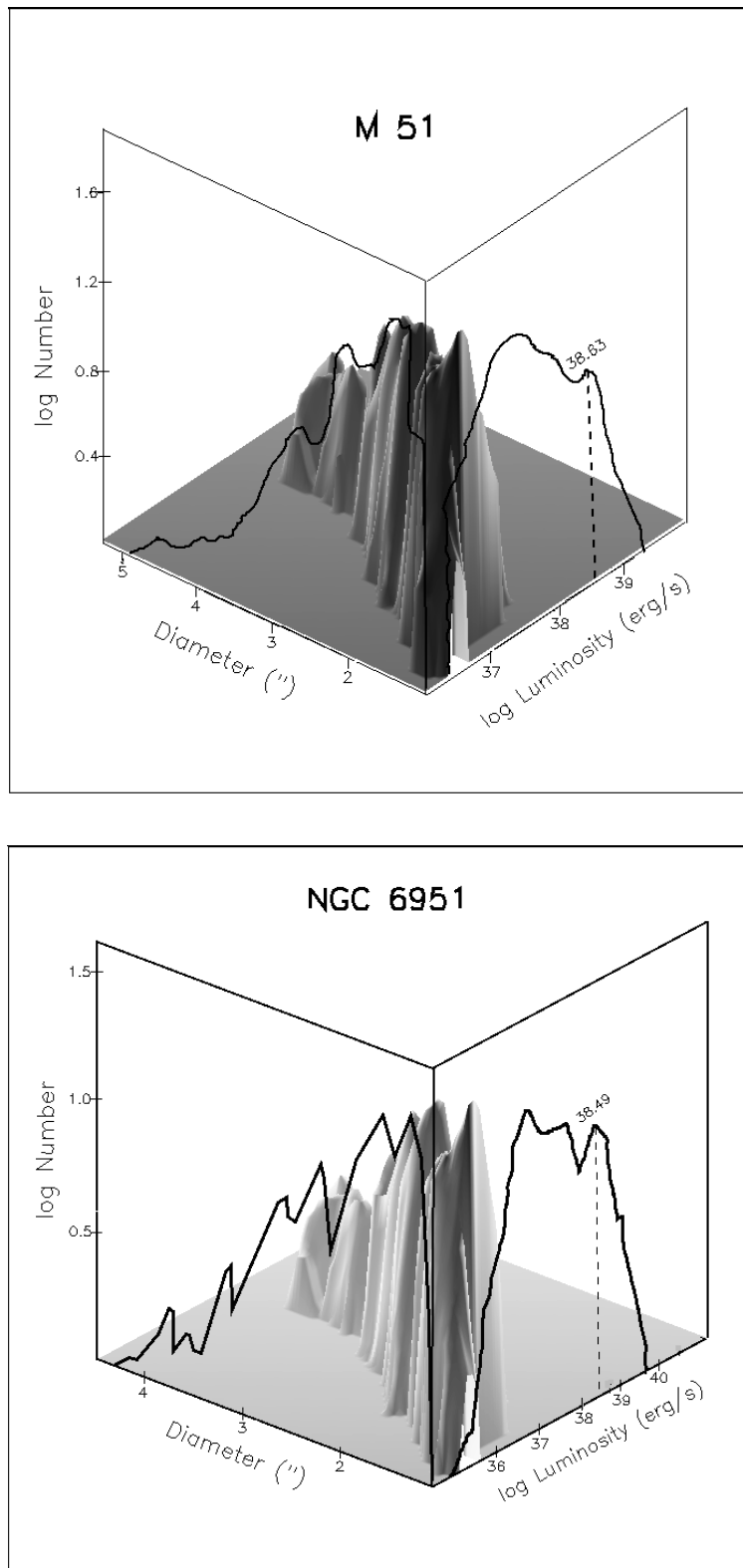


FIG. 1.—Continued

would not, perhaps, want to draw any striking conclusions from the presence of a peak no higher than 2σ . However, the peaks occur in a number of galaxies, and the chance that the peaks are the only such feature at very similar luminosity is very small for purely statistical reasons, less than 1 part in 10^3 , so it would be very hard to dismiss the peaks as statistical artifacts. That the peaks and gradient changes

occur at the same luminosity within 0.07 mag for galaxies whose distances cover a range of more than a factor of 3 also argues strongly against an observational effect (e.g., limitation in angular resolution) as their cause.

A qualitative explanation for the presence of the glitches in the LFs in terms of the transition from ionization bounding to density bounding is as follows: In a hypothetical set

of star-forming clouds with identical cloud masses but with star clusters of different integrated ionizing luminosities forming inside them, some of the clusters may be massive enough to emit more than sufficient numbers of ionizing photons than are required to fully ionize their placental clouds. In that case, whatever the intrinsic LF of the resulting H II regions (measured in ionizing photons) might be, the LF observed in H α would show a spike at the upper bound of the observed luminosity range, because any regions with extra ionizing photons would lose the excess by density bounding. In this extreme (not, of course, realistic) case we would not find a glitch but a delta function in the LF. Cloud masses are not, however, identical. To yield a glitch, two entirely plausible physical conditions are required. One is that the mass of massive stars rises statistically with the cloud mass; the other is that this rise is sufficiently steep that at and above a critical cloud mass there are sufficient Lyman continuum photons to ionize the whole cloud. We will see in § 3 that the evidence that does exist in the literature is fully consistent with these two conditions.

2.1.1. Modeling the Luminosity Functions

Here we show, using a set of fairly schematic models, that the process of density bounding ought to give rise to the form of the LF observed in H α and that the other hypothetical causes modeled for the observed behavior are in no way as plausible. The model starts by generating an artificial LF, using a population of 1000 H II regions distributed in bins of uniform logarithmic width; we chose 0.2 dex for the illustrations here as this is our preferred plotting scale for the observations. The number of regions per bin, n , is given by

$$\frac{dN}{d \log L_{\text{H}\alpha}} = n(L_{\text{H}\alpha}) = \frac{L_{\text{H}\alpha}^{\xi}}{A'}, \quad (1)$$

where $L_{\text{H}\alpha}$ is the luminosity in H α and the index ξ can be varied, but in our figures we will keep this at an observationally typical value of -1.5 . The constant A' is adjusted to normalize the number of regions at $\log L_{\text{H}\alpha} = 38$ ($L_{\text{H}\alpha}$ in ergs per second) in the 0.2 dex bin to 100. Equation (1) is the most direct way to represent the luminosity function, but conventionally either differential or logarithmic forms are used for convenience. These are respectively

$$dN(L_{\text{H}\alpha}) = \frac{L_{\text{H}\alpha}^{-\alpha}}{A} dL_{\text{H}\alpha}, \quad \frac{dN}{d \log L_{\text{H}\alpha}} = \frac{L_{\text{H}\alpha}^{1-\alpha}}{A'}, \quad (2)$$

where $\alpha = 1 - \xi$ and $A = A'/\log e$. The first part of equation (2) will be used in the development of § 3.

With the basic function of equation (1), we can apply processes that simulate the different physical effects expected to affect the LF. In the first place, we show a simulation of the effects of density bounding. The model assumes that the observed luminosity of a region in H α is reduced to $L_{\text{H}\alpha}$, above the critical value of $L_{\text{H}\alpha}$, namely, L_{Str} , at which an H II region is just fully ionized, by a factor that depends on the ratio of the true ionizing luminosity (L_i) to the ionizing luminosity that produces $L_{\text{H}\alpha} = L_{\text{Str}} = L_{i,\text{Str}}$. This is a fair parametric representation of what is predicted when the ionizing flux overflows the H II region. The formula for this is just

$$L_{\text{H}\alpha} = L'_{\text{H}\alpha} (L_i/L_{i,\text{Str}})^k, \quad (3)$$

where $k < 0$ and $L'_{\text{H}\alpha}$ is the H II region luminosity in H α if all the ionizing photons are absorbed. Given the dependence of the observed H α luminosity of a region on its intrinsic ionizing luminosity, we can transform numerically to obtain the corresponding LF in H α . Applying this to the part of the LF given by equation (1) in the range $L_{\text{H}\alpha} > L_{\text{Str}}$ (for $L_{\text{H}\alpha} < L_{\text{Str}}$, $L_{\text{H}\alpha} = L'_{\text{H}\alpha}$) with a smoothing function of Gaussian type with $\sigma = 0.1$ dex in luminosity (to correspond to the binning of the observational data), we obtain curves of the type shown in Figure 2. We can see here that the general functional form of our observations is reproduced, notably the glitch in the LF, as well as the increase in (negative) slope for $L_{\text{H}\alpha} > L_{\text{Str}}$. We can also see that the luminosity of L_{Str} is almost independent of the slope, ξ , of the initial trial function, which represents the intrinsic slope of the LF and essentially reflects the slope of the initial mass function (IMF) for massive exciting stars within the region, i.e., the glitch peak luminosity should depend little on the IMF if the break is due to density bounding, as we suggest.

To examine another possible cause of the break and the glitch in the LF, we assumed that the H II regions contain an admixture of dust, causing extinction in H α . Dust is a well-explored feature of the interstellar medium, and the main doubt is the extent to which it survives under the extreme conditions in an ultraluminous H II region. For the purpose of this exercise, we assumed a constant dust-to-gas ratio and uniform mixing, which is the case most favorable to the hypothesis that dust extinction is the cause of the LF break. This was treated by modifying the intrinsic H α luminosity $L'_{\text{H}\alpha}$ given by equation (1) [$n(L'_{\text{H}\alpha}) = (L'_{\text{H}\alpha})^{\xi}/A'$], to a resultant observed luminosity, $L_{\text{H}\alpha}$, according to the expression

$$L_{\text{H}\alpha} = (L'_{\text{H}\alpha})^{-\tau}, \quad (4)$$

where τ is an optical depth in H α given by $\tau = Br$ and the constant B takes values that normalize the extinction as follows: at radius $r = 100$ pc a region has an intrinsic luminosity $L'_{\text{H}\alpha} = 10^{38}$ ergs s^{-1} (chosen as a representative value from the observations), which is proportional to its volume, $V = (4/3)\pi r^3$ (again a dependence taken from the observations, to first order), and then B is varied at will to yield values of τ in simple decimal intervals.

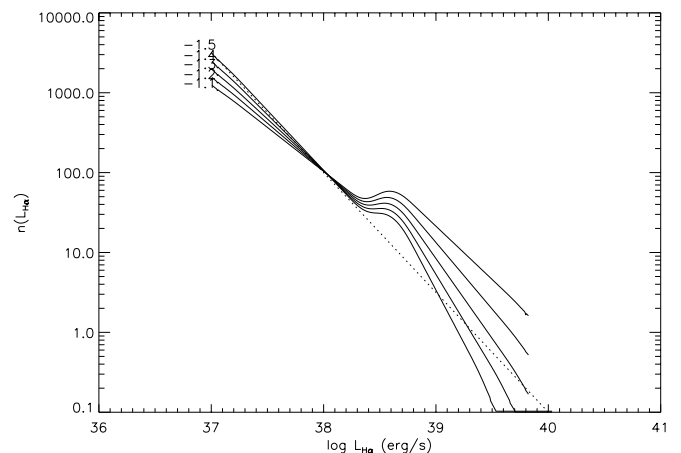


FIG. 2.—Computed models showing how the phenomenon of density bounding above a critical luminosity can lead to the observed glitch and a change of slope in the LFs of the H II regions of a disk galaxy (see text for details). Labels on contour plots indicate the intrinsic slope of the initial LF. The dotted line shows an LF with slope -1.5 before modeling the effect of density bounding.

In Figure 3 we can see the results of this modeling exercise for different values of τ at $\log L_{\text{H}\alpha} = 38$ ($L_{\text{H}\alpha}$ in ergs per second). The results show qualitatively very different LFs from what we observe. If the optical depth is small, the effect is to curtail the LF but not to alter its slope. If the optical depth is larger, the effect is to curtail the LF with a high peak and a drop to zero at a cutoff luminosity without altering the slope of the main LF.

Although the result of this exercise with dust suggests that dust extinction is unlikely to be the cause of the LF we observe, it does point to a possibility that at least qualitatively might produce an LF not unlike that observed. If dust is mixed within the H II regions having up to some limiting luminosity but then is expelled in those having higher luminosity, it may be possible to modify the curves in Figure 2 to displace some of the H II regions accumulated in the rising tail of the LFs in Figure 3 to higher luminosities, yielding an LF of the form observed. While this scenario is not physically ruled out, it would give rise to a dependence of the central H α surface brightness of the H II regions on radius that is very different from that observed, as we will explain below, and this is sufficient reason for us not to accept it as the explanation for the LF observations.

Finally, we numerically modeled another possible scenario for the break in the LF. Could it be caused by the overlapping of H II regions of a certain minimum size? In constructing the H II region catalog, one of the difficulties to overcome is that many H II regions appear to overlap on the image. We adopted the solution proposed in Rand (1992), counting each peak in H α as a single H II region. The flux of each H II region was then estimated by integrating over the pixels that could be reasonably attributed to a given region. One will undoubtedly miss a number of H II regions that are too weak to be detected in the vicinity of stronger emitters close by. This will influence the lower end of the LF but is not a significant factor in determining the true LF at the higher luminosity end (Rand 1992). Anyway, to check directly whether the overlapping cloud causes the break in the LF, we applied a new model. First we assumed the function in equation (1) as the intrinsic LF. To take care of the weaker regions in a very realistic way, we used equation (1) for luminosities between 10^{40} and 10^{37} ergs s^{-1} , and

below this limit we used a flat distribution function ($\xi = 0$ in eq. [1]), following the observed distribution in M31 by Walterbos & Braun (1992). In the computations we allowed the luminosity of a region merged with others to reach an upper limit of 10^{42} ergs s^{-1} , corresponding to the luminosity of the regions formed by the mergers. The distribution was separated into 300 discrete bins of equal logarithmic width, and the volume of H II regions per bin was calculated by simple summation, normalizing the system so that an H II region of radius 100 pc had an H α luminosity of $\log L_{\text{H}\alpha} = 38$ ($L_{\text{H}\alpha}$ in ergs per second) and by calculating the volumes in the first instance at infinite spacing between regions, i.e., with no overlaps. For each bin, the luminosity was proportional to the summed volume of regions in the bin, as we found observationally for the regions below $\log L_{\text{H}\alpha} = 38$ ($L_{\text{H}\alpha}$ in ergs per second). The total volume of all the regions is V_c .

In the model, we put the regions whose integrated volume is V_c into an enclosure of volume V , so the overall filling factor is V_c/V . The initial distribution is considered in finite-luminosity (i.e., volume) bins, indexed by i and j , where both i and j can vary from 1 to 300. Interaction of the pair of clouds, one in bin i and the other in bin j , is considered first. The probability per unit volume, P_j , of a small cloud being absorbed in a larger one is the filling factor of the clouds in bin j , which is the same as using the rule that when two clouds are sited with the distance between their centers less than the radius of the larger, the smaller is absorbed into the larger, and the volume of the resulting H II region is the sum of the volumes (and luminosities) of the two. The mean initial spacing is determined by the chosen value of V_c/V . We obtain for P_j

$$P_j = N_j V_j / V, \quad (5)$$

where N_j is the initial number of clouds within j , so the number, δN_f , of clouds affected is just

$$\delta N_f = N_i N_j V_j. \quad (6)$$

We then adjust the luminosities in proportion to the revised numbers of clouds in each bin, using the following relations:

$$N'_i = N_i - \delta N_f, \quad N'_j = N_j - \delta N_f, \quad N'_k = N_k + \delta N_f, \quad (7)$$

in which the total volume and luminosity are conserved, while the regions affected by merging are transferred to the appropriate bin of higher luminosity. This procedure is carried out in order of increasing bin luminosity so that the merged regions participate in further mergers if they are close enough to other regions. In a single pass combining all pairs of bins, the new LF is computed. Modeling the mergers in this way, we assume that H II regions are not optically thick, so that only genuine three-dimensional overlaps, not projected overlaps on the plane of the sky, need to be taken into account. As will be deducible by considering Figure 4, assuming optical thickness would only accentuate the disagreement between this type of model and the observed LFs. In Figure 4, it is clear that not only is there no evidence of a glitch, but the negative slopes of the IMFs of the merged models become less steep at high luminosities, in direct contrast to the observations. While it might be possible to find some clustering model that would yield an LF similar to those observed, its inputs would have to be very finely tuned and would be unlikely to reflect the realistic astrophysical conditions.

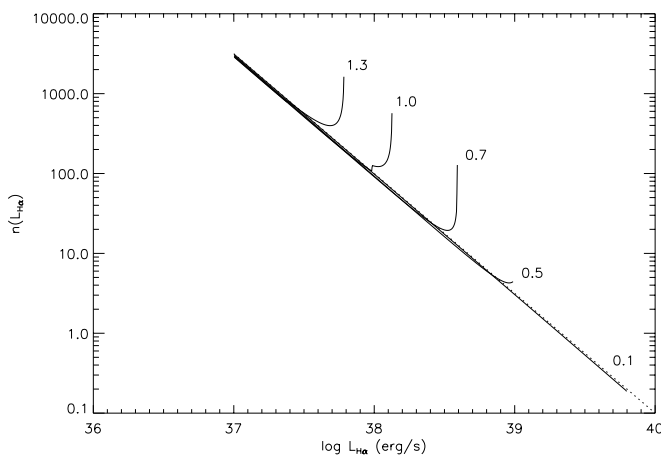


FIG. 3.—Computed models of H II region LFs with constant gas-to-dust ratio. Each solid curve corresponds to a value of integrated dust optical depth (at the H α wavelength) for a region with emitted H α luminosity of $\log L_{\text{H}\alpha} = 38$ ($L_{\text{H}\alpha}$ in ergs per second). The dotted curve represents the unextinguished LF.

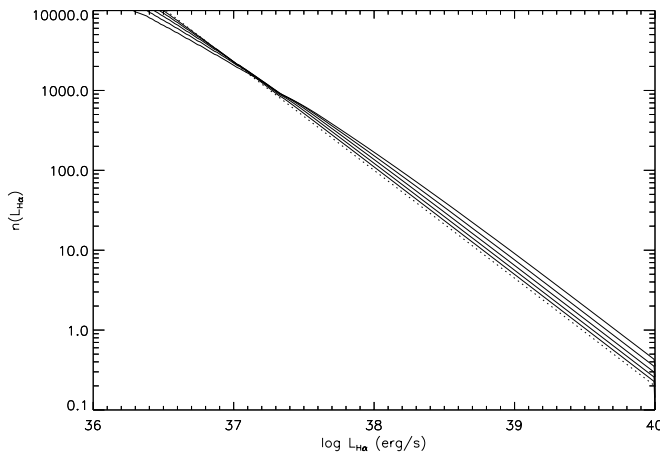


FIG. 4.—Models of the LF in H α in which increasing degrees of overlapping and absorption take place between H II regions (see text for details). Although we place little stress on the quantitative results, we can see qualitatively that the effect of assimilating regions within others is to reduce the LF slope at high $L_{\text{H}\alpha}$, not to increase the slope as observed.

In the light of the comprehensive theoretical study of LFs in H II regions, notably in the Galaxy, but with commentary on other galaxies, by McKee & Williams (1997, hereafter MW), we should add here that the effect of density bounding on the LF in H α that we claim here must function independently of almost any detailed consideration of the IMF's of the stars that ionize the regions or of its temporal evolution. The truncation of the IMF at high stellar mass, adduced by MW to explain an observed sharp steepening of the LF slope of H II regions, does not conflict with the results presented here for two reasons. First, the phenomenon explained by MW occurs at an H α luminosity almost an order of magnitude below the glitch we find. In the present study, this would be very difficult to distinguish from the rather rapid change in slope just above $\log L_{\text{H}\alpha} = 37$, because of the increasing incompleteness of our statistics at low luminosity, but in any case it is clear that one is dealing with two different real observable effects. Furthermore, a truncation of this type does not readily give rise to a

glitch in the LF, nor can it yield as a natural consequence the observed sharp increase in internal brightness gradients and central surface brightness with luminosity, described below in § 2.2. Thus neither the observations nor the model of MW relate to the same phenomenon as the one we describe here.

2.2. Central Surface Brightness and Internal Brightness Gradient

Further evidence for a change in physical regime at the H α luminosity, L_{Str} , comes from measurements of the surface brightnesses of H II regions. The observations used are the same as those for the LFs, photometrically calibrated CCD images of galaxies taken through an appropriately redshifted H α filter, with stellar continuum subtraction using a neighboring off-band filter. All observations were taken with the 4.2 m William Herschel Telescope on La Palma, and details of the observations and the reduction procedure can be found in Rozas et al. (1996a). The absolute H α fluxes and mean radii were found for several hundred H II regions in each galaxy. The largest, most luminous, and isolated were selected for profile measurements, as these subtend angles large enough to obtain reliable profile fits; a minimum radius of 5 pixels was chosen. This corresponds to the H α luminosity $\log L_{\text{H}\alpha} = 38$ in the farthest galaxy observed. The number of regions per galaxy that could be used for these measurements was in the range 30–35. Two characteristic parameters were derived per region, the central surface brightness and the mean internal surface brightness gradient (this latter was also treated in Rozas, Castañeda, & Beckman 1998a).

In Figure 5a we show the central surface brightness, S_c , as a function of $L_{\text{H}\alpha}^{1/3}$, the cube root of the H α luminosity. For spherical ionization-bounded regimes with constant density and filling factor, S_c should be proportional to the radius of a region, and as luminosity is proportional to volume, S_c should vary linearly with $L_{\text{H}\alpha}^{1/3}$. We can see from Figure 5a that for regions with luminosities below $L_{\text{H}\alpha} \sim L_{\text{Str}}$, this relation holds rather well, but for luminosities above this value there is a clear and sharp departure from proportionality. In Figure 5b we show a brightness gradient parameter,

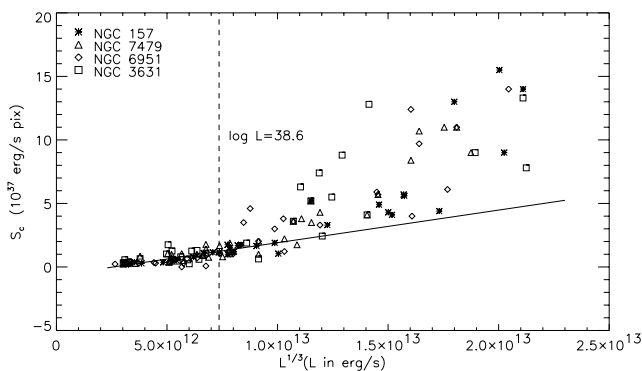


FIG. 5a

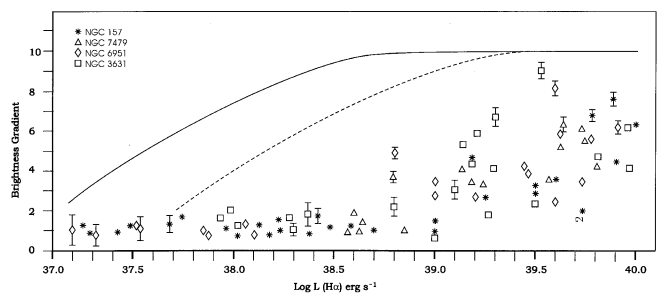


FIG. 5b

FIG. 5.—(a) Central surface brightness, S_c , in H α vs. the cube root of the H α luminosity, $L_{\text{H}\alpha}^{1/3}$, for H II regions in four galaxies selected for minimum spatial blending with neighboring regions. Below $L_{\text{H}\alpha}^{1/3} = 7.5 \times 10^{12}$ there is a good linear fit to the data, predicted for ionization-bounded regions with a constant product of density, electron density, and filling factor. Above this value there is a clear change of regime; S_c rises much more sharply with $L^{1/3}$ and the scatter widens considerably. This change must be caused by a change in the interactive behavior of gas and stars and cannot be due only to changes in stellar content or evolution within the regions concerned. (b) Radial gradient parameter, the ratio of the central surface brightness of a region to its estimated radius, in linear units. Near-constant gradients are found for $\log L_{\text{H}\alpha} < 38.6$, and strongly increasing values with increasing scatter are found for higher luminosities. The curves show the ratios of observed to intrinsic gradient for the two extremes of seeing-limited resolution (0.8 and 1.5) during the observation. A set of regions with intrinsically constant gradients would show observed gradients tending to a constant value at high $L_{\text{H}\alpha}$ rather than the steeply rising gradients observed.

obtained by dividing the central surface brightness of a region by its linear radius projected in the plane of the galaxy, plotted versus $L_{\text{H}\alpha}$. We can see that below $L_{\text{H}\alpha} = L_{\text{Str}}$, this parameter varies very little within the limits of error, while above this luminosity it tends to rise. Although the scatter also increases, the trend to higher values is clear, and the ratio of this gradient parameter above L_{Str} to the constant value below L_{Str} reaches 10 in the steepest cases and is greater than 3 in most regions with $\log L_{\text{H}\alpha} > 39$. The change in behavior seen in Figures 5a–5b could not be due to the finite resolution of the images. It is easy to show that for a hypothetical set of regions with constant intrinsic brightness gradient the observed parameter, if degraded by instrumental resolution, would tend asymptotically to a constant value at large radii, i.e., at high luminosity. This is just the reverse of what we measure: a tendency to a constant value at low luminosity. If, on the other hand, the intrinsic gradient were in fact decreasing with increasing luminosity, it would take a “conspiracy” to flatten the plot at low $L_{\text{H}\alpha}$ (i.e., an inadequate deconvolution folded with an intrinsic fall would need to cancel neatly, yielding a level plot), and the result would disagree even more strongly with the observations at high $L_{\text{H}\alpha}$. It would be very surprising to find the observed change of gradient at a similar luminosity for all the galaxies sampled if it were due to a resolution effect, since they are at quite different distances, so the linear resolution on the galaxy disk corresponding to the angular resolution of the telescope differs from object to object. The observed changes in the value of the gradient above $L_{\text{H}\alpha} = L_{\text{Str}}$ are way outside the most pessimistic error bars, so that Figures 5a–5b offer prima facie evidence of a change in physical parameters close to $L_{\text{H}\alpha} = L_{\text{Str}}$. The regions below this luminosity obey a linear volume-luminosity relation, while those above it in general do not. This break in the geometric properties of the regions cannot be explained plausibly in terms of the collective properties of the ionizing stars. It is easy to show (it was shown by Strömgren himself) that for an H II region forming within a medium of uniform density (and, we should add here, constant filling factor), the volume ionized is proportional to the rate of emission of ionizing photons, so that the geometric distribution of the brightness within a region will not depend on the number of its ionizing stars, provided that they are concentrated in a cluster near the center (certainly true for all the regions studied in this section, which have radii well over 100 pc). The observed changes must be due to the behavior of the surrounding gas. We will discuss in § 3 how these changes might occur for the observed regions.

A further point of interest here is that the constancy of the brightness gradient parameter and the dependence of the central surface brightness on $L_{\text{H}\alpha}^{1/3}$ below $L_{\text{H}\alpha} = L_{\text{Str}}$ are not consistent with the dust model that we described in § 2.1 as a testable alternative scenario for the observed behavior of the LF. Dust extinction increasing linearly with the radius of the H II region and causing a notable bump in the LF close to $\log L_{\text{H}\alpha} = 38.6$ would have an effective value of optical depth $\tau_{\text{H}\alpha}$ (at H α) close to 0.6 at our normalization value of $\log L_{\text{H}\alpha} = 38$, while $\tau_{\text{H}\alpha}$ would be 0.4 at $\log L_{\text{H}\alpha} = 37.5$ and 0.9 at $\log L_{\text{H}\alpha} = 38.5$. The surface brightness gradient would show an easily detectable systematic fall between 37.5 and 38.5, by a factor of order 2, rather than remaining constant as observed. If above $L_{\text{H}\alpha} = L_{\text{Str}}$ the observed increase in the surface brightness were due to dust being dispersed in these regions (perhaps by extra radiation

pressure), the gradient would not increase by factors of 3 to 10 from its value at $L_{\text{H}\alpha} = L_{\text{Str}}$ but at most by a factor of 2, and in any case it would never rise above the asymptotic value at small $L_{\text{H}\alpha}$, a rise that is dramatically observed. Very similar considerations hold for the central surface brightnesses. We will see in § 4 that the diffuse H α observed in the disks of our galaxies offers more direct evidence that ionizing radiation is in fact leaking out of the luminous H II regions, and this argues against major dust extinction in these regions.

2.3. Internal Velocity Dispersion of the H II Regions

The evidence discussed in the present subsection does not refer to the same set of galaxies as those treated in the bulk of the paper because the kind of data required, Fabry-Perot mapping of a galaxy in an emission line, is in no way as easy to obtain as the narrowband imaging on which the majority of our deductions are based. We have, to date, analyzed Fabry-Perot maps in H α of the disks of only two galaxies, obtained in a program of diskwide kinematics not aimed principally at the properties of H II regions. However, the statistical results on the internal velocity dispersions of the H II regions observed are of such relevance to the present discussion that it is important to include them here. They were made with the Taurus instrument on the 4.2 m William Herschel Telescope on La Palma. Details of the observations and reduction are presented elsewhere (Rozas, Sabalisk, & Beckman 1998b). We present the data here for two galaxies, M100 and M101. We had absolute flux calibrations for the regions in M100, obtained by our group in a parallel context (Knapen 1998), but for M101 we have no such absolute fluxes, nor are they available in the literature, so we give the results in relative flux units. This still allows us to infer the essential relations between flux, $L_{\text{H}\alpha}$, and the internal velocity dispersion, σ , for the regions of M101.

Figure 6a is a plot of $\log L_{\text{H}\alpha}$ versus $\log \sigma$ for the principal components of the brightest H II regions in M100. Only the brightest 10%, some 200 of the almost 2000 regions whose absolute fluxes and diameters had been determined (Knapen 1998), were bright enough to yield velocity profiles with signal-to-noise ratios high enough to give well-measured values of σ from single-frame exposures. We also have a lower limit cutoff in σ of 10 km s^{-1} , due to the combined uncertainties in the instrumental profile and the natural and thermal broadening contributions. At first glance, Figure 6a is little more than a scatter diagram, and any attempt to put a linear or even a polynomial or spline fit through the points yields little of value. One might be tempted to conclude that the horizontal spread is a little less than the vertical spread, so that a line of high gradient, perhaps akin to the prediction based on the assumed virial equilibrium of the H II regions (Terlevich & Melnick 1981),

$$\log L_{\text{H}\alpha} = 4 \log \sigma + c, \quad (8)$$

could be brought to fit the points, but there is no real justification for such a fit. However, there is one locus of regularity in these points, namely, the upper envelope of minimum σ , which can be well fitted by a straight line of slope 2.6 ± 0.14 . It is worth comparing this with the linear fit to the $\log L_{\text{H}\alpha}$ – $\log \sigma$ plot for the H II regions in M100 by Arsenault, Roy, & Boulesteix (1990), made using an observational technique similar to ours. In their case, they selected the regions of greatest surface brightness rather than an envelope of minimum σ . This coincidence is very significant

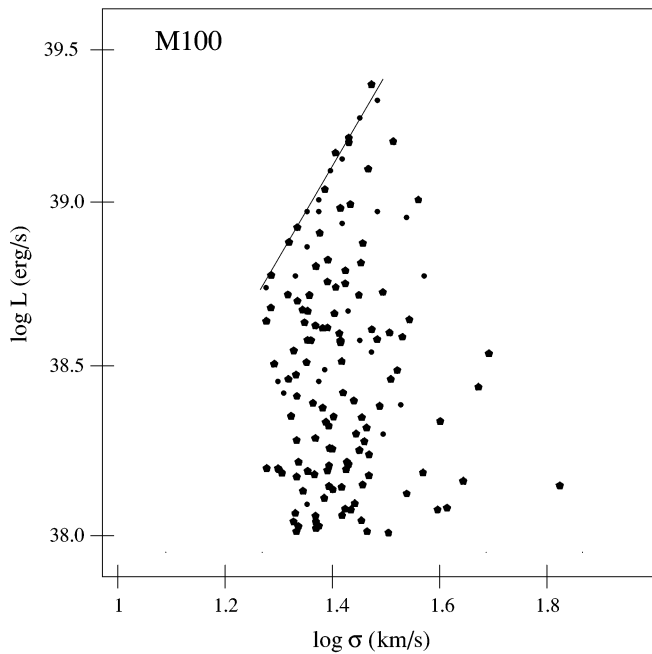


FIG. 6a

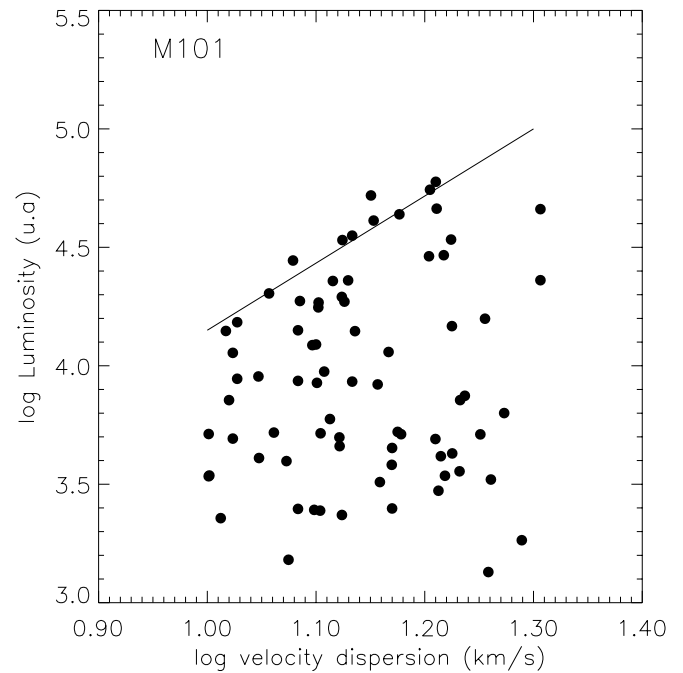


FIG. 6b

FIG. 6.—(a) Plot of $\log L_{\text{H}\alpha}$ vs. the logarithm of velocity half-width, $\log \sigma$, for the most intense emission components from the H II regions in M100, observed using the Taurus Fabry-Perot spectrometer. The linear fit is to the upper envelope of the plot, which should represent the locus of virialized regions. The slope is not 4, as predicted for ionization-bounded models, but 2.6, in agreement with density-bounded models for regions with $\log L_{\text{H}\alpha} > 38.6$. The same slope was measured by Arsenault, Roy, & Boulesteix (1990) using highest surface brightness rather than lowest σ as a selection criterion, in full accord with the hypothesis of density bounding. (b) Plot of $\log L_{\text{H}\alpha}$ vs. $\log \sigma$ for the principal emission components in M101, from a Taurus data cube without absolute flux calibration. An envelope at high $L_{\text{H}\alpha}$ and low σ , similar to that for M100, is found, with a slope calculated at 2.55, in accord with the hypothesis that the most luminous H II regions in M101 are density bounded.

physically, as we will show in § 3. In Figure 6b we show a similar $\log L_{\text{H}\alpha}$ - $\log \sigma$ plot for M101. Although the luminosity is not on an absolute scale, as explained above, we can see here also the linear envelope of what would otherwise be a scatter diagram. The best-fit measured slope to this is 2.55 ± 0.15 , and the display of points in the graph is similar to that in Figure 6a, with a slight trend for the σ -values to occupy a wider range at lower luminosities.

Our interpretation of the observations in Figures 6a–6b is that in general the internal velocity dispersions of the H II regions as shown in their H α emission line profiles are not in virial equilibrium. Whatever the mechanisms for transferring energy to the ionized gas (it is beyond the scope of the present article to consider these), it is reasonable to assume that the emission-line width for an arbitrary region will be enhanced by the presence in the gas of undamped effects of the outflowing winds from massive stars or even of supernova explosions. In the region NGC 604 in nearby M33, Sabalisck et al. (1995) showed the morphological complexity of the velocity field. The principal velocity component for a more distant region observed with our technique is a luminosity-weighted sum, which must incorporate any discrete burst of input energy and should not in general fit a virial equilibrium relation. In this scenario, regions showing the lowest value of σ for a given luminosity will be those whose emission profiles are least affected by nonvirialized energy injection, so that regions closest to virial equilibrium should lie on or near the low- σ envelope of the $\log L_{\text{H}\alpha}$ - $\log \sigma$ relation. Physically, it is plausible that the most massive regions will most rapidly

damp the bursts of injected energy, so that in the full ($\log L_{\text{H}\alpha}$, $\log \sigma$)-diagram an increasing fraction of regions will be found on the virial envelope with increasing mass (and hence luminosity). The linear envelopes in Figures 6a–6b can thus be identified as the loci of those regions whose $\log L_{\text{H}\alpha}$ - $\log \sigma$ relation should obey the conditions of the virial theorem.

It is therefore very significant that the slopes of these envelopes are ~ 2.5 and not 4, as predicted for virialized systems (see, e.g., Terlevich & Melnick 1981; Tenorio-Tagle, Muñoz-Tunón, & Cox 1993), since the value of 4 follows from assuming the conventional picture of ionization-bounded regions. The regions on the envelope in Figure 6a all have luminosities greater than L_{Str} , so we would expect them to be density bounded, and we will show below that a slope close to 2.5 is in the range predicted for virialized regions that are density bounded. Arsenault, Roy, & Boulesteix (1990) performed an exercise similar to ours for the H II regions of M100, but they selected a small number of regions of maximum surface brightness for their $\log L_{\text{H}\alpha}$ - $\log \sigma$. The slope of their graph, 2.6, confirms our scenario, as we have shown above that the regions of highest surface brightness are found in the range $L_{\text{H}\alpha} > L_{\text{Str}}$, where the regions are most massive, where the virial relation should hold in the ionized gas, and where our theory predicts density bounding.

In this section, we have presented evidence for a change in the physical properties of the H II regions in spirals in the very high luminosity range (termed “giant H II regions” by Kennicutt et al. 1989) above $L_{\text{H}\alpha} = L_{\text{Str}} = 10^{38.6}$ ergs s $^{-1}$ in

H α . We have argued, based firmly on observation, that this may mark a “phase change” from ionization bounding to density bounding. In the next section, we argue from scaling calculations that this type of change is physically plausible.

3. WHY SHOULD VERY LUMINOUS H II REGIONS BE DENSITY BOUNDED?

3.1. Luminosity Function

In § 2.1, we outlined what would be required of the relation between the mass in high-mass stars within a star-forming cloud and the mass of the cloud itself so that the H II regions with luminosities above a specified value were density bounded, while those below this value were ionization bounded. The relation is that the mass in ionizing stars should, with cloud mass, grow quickly enough for the ionizing flux to rise more quickly than the cloud mass. In the very schematic model we present below, we assume, to simplify the argument, that the average cloud density does not vary, an assumption that holds well, observationally, for regions up to the transition. The model will not fail physically if this condition is not well maintained at higher luminosities, but the simplicity of the quantitative inferences will be lost.

Let the ionizing flux, L_i , from an H II region depend on the total stellar mass, M_* , in ionizing stars within the region according to

$$L_i = kM_*^\alpha, \quad (9)$$

where k is a constant. We can set observational constraints on α . From the semiempirical study by Vacca, Garmany, & Shull (1996) we find that the rate of emission of Lyman continuum photons from OB stars rises approximately as the square of the stellar mass. The index falls from values higher than 2 for early B and late O stars to values close to 2 for O3 stars. For a uniform Salpeter IMF slope without a physical cutoff in stellar mass at the upper mass end with increasing placental cloud mass, the weighted mean index for a young star cluster would be a little over 2, and this would be the appropriate value for α . If, however, there was a fixed physical stellar mass limit, rather than a statistical limit for each cluster, α would be unity or close to unity. Although evidence on this point is not abundant, Massey & Hunter (1998) measured with *HST* the photometric properties of the most massive stars in the cluster R136, which ionizes the very luminous H II region 30 Doradus in the LMC. They found, inter alia, that the IMF slope appears to retain its Salpeter value of -2.35 to the highest masses and that there is no obvious evidence for an upper mass cutoff; they find stellar masses ranging well over 120, through 130, and up to $150 M_\odot$. Without generalizing unduly or being especially optimistic, it is reasonable to infer that α , though not necessarily greater than 2, will generally be higher than 1, and we will say provisionally that α should be between 1 and 2.

Now we let the mass M_* in stars contributing significantly to the ionization depend on the placental cloud mass M_{cl} according to

$$M_* = jM_{cl}^\epsilon, \quad (10)$$

where j is a constant. There is not very much direct evidence on the value of ϵ . Larson (1982) reported from a compilation of observations within the Galaxy that the highest

mass of a young cluster varies as the placental cloud mass to the power 0.43. If we take the IMF slope as -2.35 , the mass of stars contributing to the ionizing photon flux rises with an index of $\sim(0.43)(2.35)$; we derive the value 2.35 as the sum of 4.35, from the mass-weighted integral of the Salpeter function, and -2 , which takes into account the effective contribution of mass to ionizing luminosity. Using Larson's result thus yields a value for ϵ of 1.01, effectively unity, for ϵ .

The condition that the rate of production of ionizing photons fully ionizes and overflows the placental cloud of a young cluster for clouds whose masses (and therefore H II region luminosities) exceed a specific value is found by combining equations (9) and (10) and is just

$$\alpha\epsilon > 1. \quad (11)$$

The empirically inferred values for α and ϵ derived above readily satisfy this condition. Although, as we have seen, direct evidence about α and ϵ is sparse, there are two indirect ways to estimate $\alpha\epsilon$ from the observations presented in the present paper, both of which confirm that $\alpha\epsilon$ must be greater than unity. One uses the gradient of the H α LF, and the other the slope of the virial envelope of the $(\log L_{H\alpha}, \log \sigma)$ -diagram.

The first estimate comes from the ratio of the slopes of the H II region LF in H α above and below the critical luminosity, $L_{H\alpha} = L_{Str}$. We can express the LF for $L_{H\alpha} < L_{Str}$ as

$$dN_1(L_{H\alpha}) = AL_{H\alpha}^{-\beta} dL_{H\alpha} \quad (12)$$

and the LF for $L_{H\alpha} > L_{Str}$ as

$$dN_2(L_{H\alpha}) = BL_{H\alpha}^{-\gamma} dL_{H\alpha}, \quad (13)$$

where A and B are constants. Inspection of Figure 7 shows that this parameterization is a good representation of the data. In the range $L_{H\alpha} < L_{Str}$ (below the transition), the functional expression for the ionizing flux is the same as that for the H α flux in equation (12) (these H II regions are ionization bounded); so that from equation (9) we can write

$$dN_1(M_*) = bM_*^{-\delta} dM_*, \quad (14)$$

where b is a constant and

$$\delta = 1 + \alpha(\beta - 1). \quad (15)$$

Combining equations (14) and (10) yields

$$dN_1(M_{cl}) = cM_{cl}^{-\eta} dM_{cl}, \quad (16)$$

where c is a constant and

$$\eta = 1 + \epsilon(\delta - 1). \quad (17)$$

By substituting equations (17) and (15) into equation (16), we have

$$dN_1(M_{cl}) = cM_{cl}^{-[1 + \epsilon\alpha(\beta - 1)]} dM_{cl}. \quad (18)$$

Equation (18) is the mass function of the clouds below the transition ($L_{H\alpha} < L_{Str}$).

If clouds with luminosities $L_{H\alpha} > L_{Str}$ are fully ionized, the slope of their mass function is also that of their luminosity function. This slope is the index γ of equation (13). At $L_{H\alpha} = L_{Str}$, the slopes of the mass functions below and

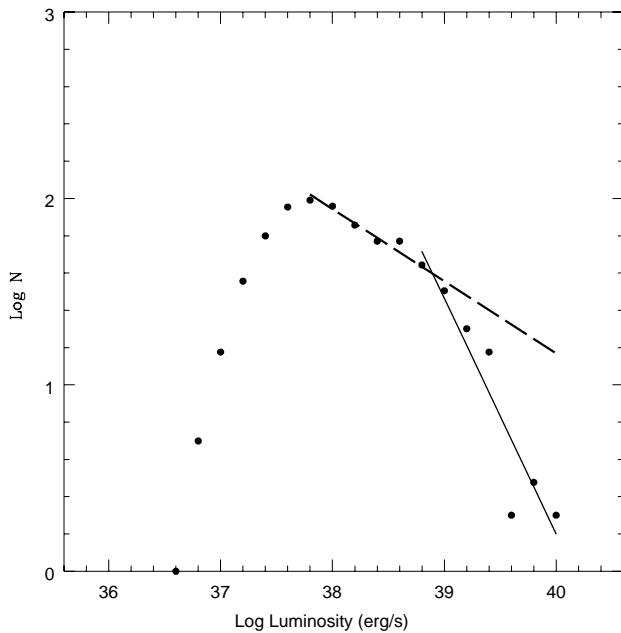


FIG. 7.—Schematic showing how the integrated ionizing flux from the luminous density-bounded H II regions in NGC 157 can be estimated by subtracting the observed LF for $\log L_{\text{H}\alpha} > 38.6$ from the extrapolated LF obtained by extending the observed function below $\log L_{\text{H}\alpha} = 38.6$ to higher values. This estimate indicates that the density-bounded regions leak sufficient Lyman continuum photons in this galaxy to ionize the diffuse medium without additional sources of ionization.

above L_{Str} should be equal, as there is no reason to predict a discontinuity in the cloud mass function. Then we can write

$$\gamma = 1 + \epsilon\alpha(\beta - 1), \quad (19)$$

which is

$$\alpha\epsilon = (\gamma - 1)/(\beta - 1). \quad (20)$$

From equation (20), we deduce that the condition $\alpha\epsilon > 1$ implies $\gamma > \beta$, i.e., that the slope of the LF in the range $L_{\text{H}\alpha} > L_{\text{Str}}$ should be steeper than the slope in the range

$L_{\text{H}\alpha} < L_{\text{Str}}$. We can see in Figure 1 that the LFs for all the galaxies observed do meet this condition; i.e., for each galaxy γ is greater than β . In Table 1 we give numerical values for β and γ for eight galaxies taken from our own work and from the literature. Since $\epsilon \sim 1$, we could use equation (20) and the measured LF in H α for a galaxy to obtain an empirical value for α . Another way to derive α is by weighting the data in Vacca et al. (1996) by the stellar IMF. Equating the two values enables us to derive the IMF slope. Using this technique, the values found lie in the range 2 to 2.5 for the LFs of the galaxies measured in the present paper. However, the method is not intrinsically very accurate, as it requires the ratio of two observables, each of form $x - 1$, where $x \gg 1$. A more reliable way to obtain the IMF slope uses the gradient of the $\log L_{\text{H}\alpha} - \log \sigma$ envelope in the velocity-dispersion diagram, as we will now explain in § 3.2.

3.2. Internal Velocity

The virialization of the gas motions within H II regions has been proposed (Terlevich & Melnick 1981) not so much as a working hypothesis but rather as a desirable case that would allow us to measure the gravitational mass of an emitting region. We showed in § 2.3 that the majority of the H II regions in the two galaxies whose $(\log L_{\text{H}\alpha}, \log \sigma)$ -diagrams are plotted are not in virial equilibrium. The H α flux they emit is a combination of individual sources within each region, some of which have nonrandom motions with relatively high velocities. Although the mass fraction in these typically expansive motions may not be high, a luminosity-weighted profile incorporates them and will always tend to have a supervirial value for its half-width. We argued in § 2.3 that the lower envelope in σ of the $\log L_{\text{H}\alpha} - \log \sigma$ distribution should correspond to the virialized regions and showed that the regions found on this lower bound in σ (which is also an upper bound in $L_{\text{H}\alpha}$), will in general be density bounded. One corollary of this is that the predicted fourth-power relationship between luminosity and σ , though good for the Lyman continuum flux of the regions on the envelope, should not hold for H α since H α does not measure the total emitted flux in this case. A first-order estimate of the appropriate index relating both the total H α emitted flux and the Lyman continuum flux can be

TABLE 1
H α LUMINOSITIES

Galaxy	$\log L_{\text{Str}}$ (L in ergs s^{-1})	β ($\log L_{\text{H}\alpha} < L_{\text{Str}}$)	γ ($L_{\text{H}\alpha} > L_{\text{Str}}$)	Reference
NGC 157	38.66	1.31	2.18	1
NGC 3359	38.60	1.44	2.10	2
NGC 3631	38.54	1.51	2.16	1
NGC 5194	38.63	1.52	2.39	3
NGC 6764	38.60	1.30	2.11	1
NGC 6814	38.69	1.67	3.39	4
NGC 6951	38.49	1.33	2.74	1
NGC 7479 (disk)	38.65	1.25	2.10	5

NOTES.—H α luminosities, L_{Str} , were measured at the peaks of the glitches for the eight galaxies for which high-quality data yield complete LFs in H α . Standard stellar calibrators were used. The distance to the objects was taken on the basis of $75 \text{ km s}^{-1} \text{ Mpc}^{-1}$ for H_0 , assuming that a measured radial velocity is due exclusively to the Hubble flow. The slopes of the LFs in H α below and above L_{Str} are given. The mean measured uncertainty in β and γ is ± 0.05 and ± 0.15 , respectively.

REFERENCES.—(1) Rozas et al. 1996a; (2) Rozas, Zurita, & Beckman 2000; (3) Rand 1992; (4) Knappen et al. 1993; (5) Rozas et al. 1999.

obtained from the scaling model in § 3.1. If the H α luminosity of an H II region above the Strömgren transition is $L_{\text{H}\alpha}$, the Lyman continuum luminosity (in units of the transition luminosity values) is

$$L_{\text{Lyc}} = L_{\text{H}\alpha}^{\alpha\epsilon}, \quad (21)$$

and, by incorporating this relation into the virial prediction, equation (8), we have

$$L_{\text{H}\alpha} = p\sigma^{4/(\epsilon\alpha)} = p\sigma^n, \quad (22)$$

where p is a constant and $n = 4/(\epsilon\alpha)$. We can see that the condition for density bounding, $\epsilon\alpha > 1$, implies that $n < 4$ and that the observed values for M100 and M101, $n \sim 2.5$, are in agreement with this condition, yielding a value of $\alpha\epsilon$ close to 1.6. Equation (22) gives, in principle, a more reliable method for measuring $\alpha\epsilon$ than the LF slope ratio in equation (20), but it requires a much higher investment in observation and reduction. If we can combine the two tests for a number of galaxies, this will give a useful quantitative check on the density-bounding hypothesis.

3.3. Stability of the Transition Luminosity

In Table 1 we list the luminosities L_{Str} of the peaks in the observed LF at the transition. The mean value of L_{Str} is 4.05×10^{38} ergs s^{-1} , which is 1.4×10^{50} photons s^{-1} . This is the equivalent of 10 main-sequence stars of type O7 or two of type O3 (Vacca et al. 1996), which should be raised by a factor of 2.23 to allow for the ratio of Lyman continuum photons to H α . The rms scatter is surprisingly low: 6.2% of L_{Str} , i.e., 0.07 stellar mag. It is important to note here that if the peaks were induced by some effect of limited angular resolution, the rms scatter would be 0.4 mag because of the range of distances of the galaxies observed, a powerful reason to reject this possibility, recently proposed by Pleuss & Heller (2000). It is interesting to compare this with the dispersion of the integrated luminosities of the same galaxies, taken from the Tully catalog (1987), which show a scatter of 0.15 mag. Although the sample is too small for us to draw a powerful conclusion, the promise of the glitch as a distance indicator is supported by the fact that its scatter is significantly lower than that of the absolute luminosities of the host galaxies in the sample under observation.

Our sample is still too small to determine whether the transition can be used as a standard candle on extragalactic scales, but it appears a priori to satisfy the four criteria proposed by Aaronson & Mould (1986) for a cosmological standard candle: it (1) exhibits small, quantifiable dispersion, (2) is measurable in enough galaxies to be calibrated locally, (3) has a well-defined physical basis, and (4) is bright enough to be used well into the region where the Hubble flow predominates. The observed peak in the H α LF for H II regions in disk galaxies promises to satisfy all four criteria. We have given here the empirical case for criteria 1, 2, and 4, and very reasonable backing for criterion 3. A criterion not brought out by Aaronson & Mould is that the observable should be permanently available to observe. This is of course not satisfied by supernovae, and although permanency is not an absolute requirement, the Strömgren transition appears to be a high-luminosity and permanent feature of disk (and probably irregular) galaxies. The initial work presented here clearly requires support from a larger sample of galaxies.

Although a purely empirically determined value of L_{Str} could, given its low scatter, be used as a standard candle, it is clearly desirable to establish the underlying physics more firmly than we have been able to do here. Nevertheless, if we can assume the transition hypothesis maintained in the present paper it does give a clear physical explanation for the low scatter in L_{Str} . Starting from equation (9) and assuming a constant cloud density (which, as explained above in § 2.2, appears valid for clouds up to and including those with $L_{\text{H}\alpha} = L_{\text{Str}}$), we can rewrite the equation in terms of the mass, M_i , of the ionized cloud as

$$M_i = k' M_*^\alpha, \quad (23)$$

where k' is a constant. The stellar mass, M_* , and the mass of the whole placental cloud, M_{Cl} , are related by equation (10). At the transition, the mass of the ionized cloud just equals the whole cloud mass, and by calling this mass M_{Str} we can find an expression for M_{Str} by combining equations (23) and (10) to obtain

$$M_{\text{Str}} = k'^{1/(1-\alpha\epsilon)} j^{\alpha/(1-\alpha\epsilon)}, \quad (24)$$

where j is the constant of equation (10).

If we take $\alpha = 1.5 = \alpha\epsilon$, the fractional variation in the mass of a cloud for a given luminosity is

$$\left| \frac{dM_{\text{Str}}}{M_{\text{Str}}} \right| = \left| -\frac{1}{2} \frac{dk'}{k'} \right| + \left| -\frac{3}{4} \frac{dj}{j} \right|. \quad (25)$$

However, in any given galaxy, the transition peak in the luminosity function is formed by a significant number of regions, which we specify as N , so that the variance in the peak luminosity is given by

$$\frac{dL_{\text{Str}}}{L_{\text{Str}}} = N^{-1/2} \frac{dM_{\text{Str}}}{M_{\text{Str}}} = N^{-1/2} \left(0.5 \frac{dk'}{k'} + 0.75 \frac{dj}{j} \right). \quad (26)$$

Since in the galaxies observed N is of order 50, $N^{-1/2}$ is of order 0.15, and it is this collective property of L_{Str} that makes it such a stable index as opposed to, say, the luminosity of the n th brightest individual H II region. We would expect the main variable influencing both k' and j to be the metallicity. The parameter j depends on the IMF, and recent results show, to the surprise of some, that apparently the metallicity hardly plays a role in determining the cluster IMF slope. The IMFs of stars in the Galaxy (Massey, Johnson, & de Gioia-Eastwood 1995a) and in the LMC (Massey et al. 1995b) with masses greater than $10 M_\odot$ are found to have slopes close to the Salpeter (1955) value of -2.35 , in spite of their large metallicity difference. In a recent review article, Elmegreen (1997) argues that this is because of the essentially fractal nature of the fractionation process leading to star formation. Whatever the physical cause, this invariant property works in favor of an invariant luminosity for the Strömgren transition.

The parameter k' , relating the number of Lyman continuum photons to stellar mass, is of course a function of metallicity, but over a range between 0.5 solar and 2 solar, calculations by García Vargas et al. (1995) show that the flux from an O star will not vary by more than a few percent, and the quantitative effect of different metallicities on the net absorption within the H II regions themselves is also small if we are looking at hydrogen ionization (the situation would be more metal dependent for helium).

In practice, to establish L_{Str} as a standard candle requires further steps: calibration locally using Cepheid distances

and the *HST* Key Project galaxies and extension of the LF database in nearby galaxies to obtain a reliable variance for L_{Str} . The potential range in z would be limited by the angular sizes of the H II regions rather than by their luminosities. A practical ground-based limit is given by the distance of an H II region with $L_{\text{H}\alpha} = L_{\text{Str}}$, which subtends $0''.5$, i.e., $2 \times 10^4 \text{ km s}^{-1}$. The use of *HST* would push this limit back considerably. Since the variance appears to be low, this extra secondary distance standard may be of use, e.g., in probing the depth and structure of neighboring galaxy clusters.

4. ESCAPING LYMAN CONTINUUM PHOTONS AND THE DIFFUSE H α EMISSION

The origin of the photons that ionize the diffuse interstellar medium relatively far from H II regions, which does not contain observable sources of ionization, has not been definitively assigned. The OB stars in H II regions are in some sense a natural source of this ionizing radiation, but doubts have arisen for two reasons. First, can enough radiation escape from the immediate environments of the OB stars, i.e., from the H II regions themselves, and, second, can

the mean free path of these photons be sufficiently long for them to ionize the diffuse medium over the full extent of a galactic disk? These doubts have led to at least one alternative model, notably that by Sciama (1990), who proposed the decay of massive neutrinos as a means of producing in situ Lyman continuum photons in the diffuse ISM. The hypothesis of density bounding for the most luminous regions can resolve the first of the two doubts (the second would have to await detailed models of the inhomogeneous ISM for its resolution). We can estimate the flux leaking out of the luminous H II region population by extrapolating the H α LF of the H II regions in a galaxy in the range $L_{\text{H}\alpha} < L_{\text{Str}}$ to the range $L_{\text{H}\alpha} > L_{\text{Str}}$ and subtracting the measured LF in this upper range. The difference should approximate the ionizing flux equivalent that escapes from the density-bounded regions. If this is greater than the measured diffuse flux, we have a *prima facie* case in favor of the model as an explanation for the latter.

We have used NGC 157 to show whether this hypothesis is worth pursuing, and Figures 7 and 8 illustrate the procedure for this galaxy. To take into account H II regions below our detectability limit, we extrapolated our LF below

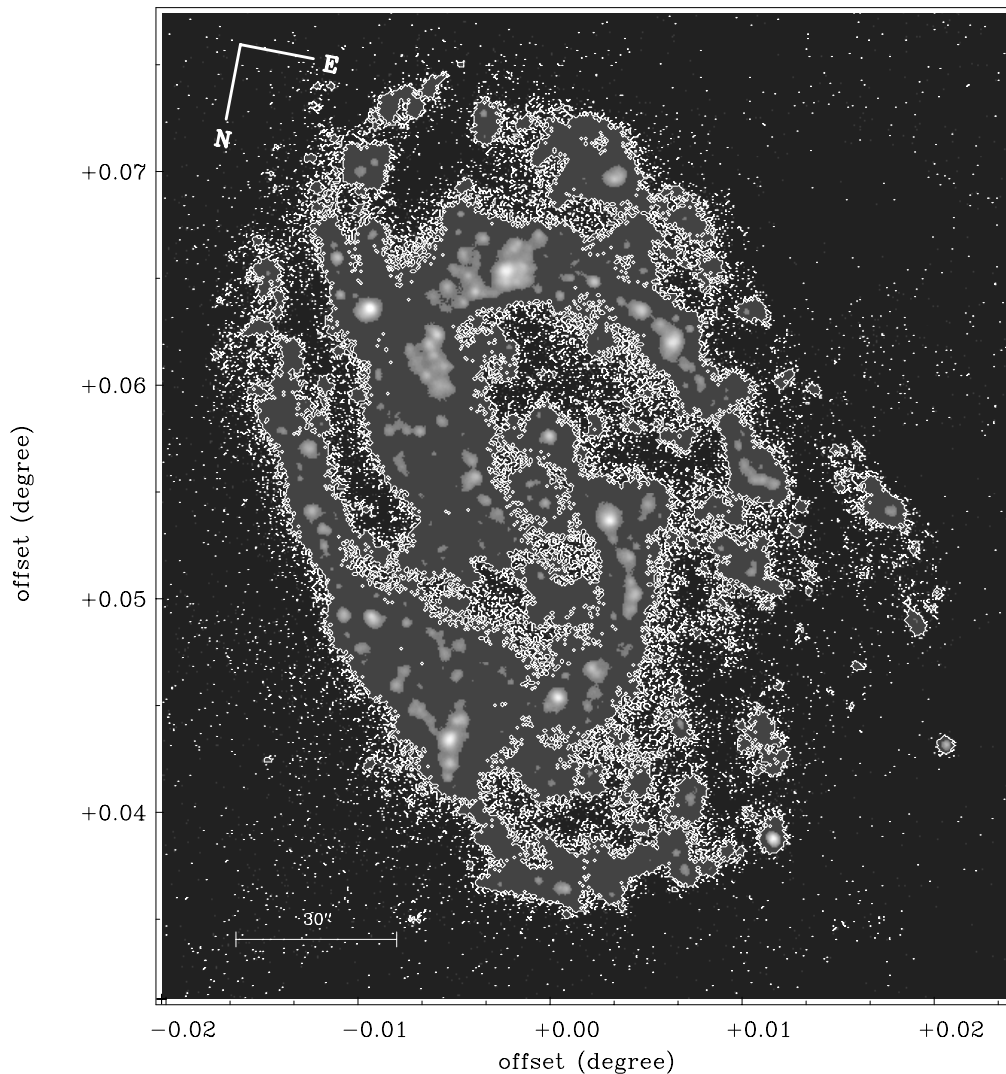


FIG. 8.—H α image of NGC 157 illustrating how the regions of highest luminosity also dominate in surface brightness and how the diffuse H α in the disk is correlated spatially with these. The major fraction of the ionization of the diffuse warm medium in disks should be due to these extremely luminous, density-bounded regions. The external isophote is at an emission measure of 7 pc cm^{-6} .

this limit, using the LF measured for M31 by Walterbos & Braun (1992), which goes down to $\log L_{\text{H}\alpha} = 35$ ($L_{\text{H}\alpha}$ in ergs per second), thanks to the proximity of M31. We scaled the measured LF for NGC 157 at $\log L_{\text{H}\alpha} = 38$, where our sample is statistically complete, and used the form of the LF from Walterbos & Braun to extrapolate to lower values. The observed truly diffuse H α flux is compared with that available because of Lyman continuum photons escaping from the density-bounded H II regions as follows:

The observed upper bound to the diffuse flux is 2.3×10^{41} ergs s^{-1} (the implied ionizing photon flux is 1.7×10^{53} Lyc photons s^{-1}).

The computed escaping flux is 3.1×10^{41} ergs s^{-1} (2.3×10^{53} photons s^{-1}).

This example shows that, for the density-bounding hypothesis, the flux escaping from the luminous H II regions is easily sufficient to yield the diffuse H α observed in NGC 157, and in a related study (Zurita, Rozas, & Beckman 2000) we are amplifying the sample treated in this way to see whether the model is as good at accounting for the diffuse H α in a wider sample of galaxies. Ferguson et al. (1996) showed that there is a good geometric correlation between the positions of H II regions in general and the diffuse flux in the two galaxies they studied in detail. It will be interesting to see if this correlation is improved when the most luminous H II regions are used, as should be the case if our model is valid. At this stage, given the clumpiness of all H II regions, we would not postulate that Lyman continuum photons cannot escape at all from regions in the range $L_{\text{H}\alpha} < L_{\text{Str}}$, only that the regions above L_{Str} should be contributing proportionally in excess of their already high measured H α output.

It is interesting that the computed escaping flux in NGC 157 is in excess of the observed diffuse flux. This difference appears to be well outside our estimates of random and systematic errors in all the quantities estimated and suggests that the down-conversion of Lyman continuum photons in the diffuse medium is by no means sufficient to soak up all the ionizing flux leaking out of the density-bounded regions. A good fraction of all the ionizing photons emitted by the OB stars must escape completely from the plane of the galaxy. If this effect is true of the majority of disk galaxies, the implication for the ionization of the intracluster medium in clusters of galaxies is of considerable potential interest.

5. DISCUSSION

We have used three types of observations to argue for a change in physical regime between ionization bounding and density bounding in H II regions at a characteristic H α luminosity close to $\log L_{\text{H}\alpha} = 38.6$ ($L_{\text{H}\alpha}$ in ergs per second), which we have termed the Strömgren luminosity, L_{Str} . They are the change of slope, accompanied by a glitch in the H α LFs of the complete H II region populations in a set of observed disk galaxies; the quantitative relation between internal velocity dispersion, σ , and H α luminosity, $L_{\text{H}\alpha}$, of the H II regions on the virial envelope of the $\log L_{\text{H}\alpha}$ - $\log \sigma$ distribution for the complete population in a galaxy; and the change in behavior of the H α surface brightness of regions in the range $L_{\text{H}\alpha} \approx L_{\text{Str}}$. Of these, the first two are presented as evidence of the kind of transition proposed, while the third, though of interest, is not as precisely defined by the observations, and its cause is at this stage fully open

to other explanations. Indeed, to sustain our basic hypothesis we will clearly require spectroscopic observations, as specified below. However, the narrow range in the luminosity of the peaks of the LFs presented here means that this feature is of considerable interest on purely empirical grounds, as a potential secondary standard candle. For this reason alone it is worth making a firm effort to understand the underlying physical behavior causing the peak and change of slope.

In § 2.1, we showed that two phenomena that could occur, which at first thought might be able to account for the LF observations (the effect of the overlapping of regions on scales commensurate with the luminosities near $L_{\text{H}\alpha} = L_{\text{Str}}$ and the effect of dust extinction within and enveloping the regions) will not give rise to the observed LF change and are not in fact viable as explanations for the observations. We ought also to consider an effect brought out by MW, who examine the relationship between the properties of H II regions within the Galaxy and their OB stellar components. They present models to explain the change in slope of the H α LF at moderately high luminosities, which they attribute to an essentially statistical effect due to the discrete number of high-luminosity stars and its relation with the total ionizing luminosity of an H II region. In their paper, MW discuss the effects of envelopes of diffuse gas around giant H II regions, which are observed for the majority of regions and which correspond to the “core-halo” structure noted in Kennicutt et al. (1989). In the present study we have taken this structure as correct and have not discussed it in further detail. The regions defined by our empirical limiting isophotal method contain the whole of the core and the halo and are clearly bigger than regions defined only by their cores or by their emission radii at radio wavelengths. It is important to note here that the change in the LF slope predicted by the MW models occurs at an H α luminosity an order of magnitude less than that of the glitch we observe. Our observations here effectively disguise the MW break because it occurs where our sample is incomplete, leading to the broad peak and decline to low luminosities, which are statistical artifacts. Neither our models nor our observations contradict the results of MW, but their work does not examine the LF gradient change at $L_{\text{H}\alpha} = L_{\text{Str}}$.

The changes that occur in the surface brightness and surface brightness gradients of the regions in the luminosity range $L \approx L_{\text{Str}}$ are clearly of interest physically, but it is not so easy for us to show that they are attributable to a transition to density bounding, although we do have significant technical advantages in resolution and signal-to-noise ratio over the observers in the 1980s (for example, the number of regions listed in Kennicutt et al. 1989 for NGC 7479 was 67, while in the data yielding the internal brightness gradients used in the present paper we cataloged over 1000 regions in this galaxy; Rozas et al. 1999). Nor can the changes in parameters presented in Figures 5a–5b be readily attributed merely to angular resolution limitations, as suggested recently by Pleuss & Heller (2000), based on their study of M101. Their argument is based on a scaling of the results from that galaxy to a distance of 20 Mpc, but the distances of the galaxies in the present sample range from 7 to 38 Mpc ($H_0 = 65 \text{ km s}^{-1} \text{ Mpc}^{-1}$), a factor of over 5 in distance. The observed increase in surface brightness and surface brightness gradients in the range $L_{\text{H}\alpha} = L_{\text{Str}}$ cannot occur for regions with constant density and filling factor, as well pointed out by M. L. McCall (1999, private commu-

nication); density-bounded regions would not show surface brightness gradients different from ionization-bounded regions if their mean densities and filling factors were invariant. Thus, although we have used the approximation of constant density and filling factor in modeling the changes in properties across the transition, it cannot hold for regions at much higher luminosities than L_{Str} . The product of density and filling factor must rise in this range. We can examine a simple case in which two H II regions have the same H α luminosity but one is ionization-bounded and the other density bounded; the factor relating the total ionizing luminosity of the density-bounded region to the fraction that is downconverted to H α we term “ g .” In a self-consistent scenario, g can represent the factor by which the product of the density and filling factor of the density-bounded region exceeds that in the ionization-bounded region. It is easy to show that the central surface brightness of the (assumed spherical) density-bounded region will be greater by the factor $g^{2/3}$, and the radial brightness gradient, parameterized as the central brightness divided by the radius, will be greater by the factor g . This exercise does not prove that density-bounded regions will necessarily have higher surface brightnesses and brightness gradients, only that the assumption of density bounding is consistent with this condition and hence consistent with our observations. To fulfill this requirement, the density, the filling factor, or both must be rising parameters above $L_{\text{H}\alpha} = L_{\text{Str}}$. While it is perfectly plausible that more intense ionizing sources produce higher filling factors and that the most massive clouds have higher mean densities, it is not obvious that these changes will not begin to occur below $L_{\text{H}\alpha} = L_{\text{Str}}$, i.e., it is not obviously a physical necessity that the surface brightness increase occur just at the transition. The fact that it appears to occur at, or near, what we believe to be the transition cannot at this stage be taken as strong support for the hypothesis of density bounding. Direct, spatially-resolved measurements of in situ electron densities made with line-intensity ratios will be required to further our understanding of this point. We must also be prepared to examine our data in the light of nonisotropic models for luminous H II regions, such as the “chimney” hypothesis (Norman & Ikeuchi 1989; Heiles 1990) discussed in more physical detail by Dove & Shull (1994), in which at a critical luminosity a region can break out of the denser disk gas into the halo. These models appear, however, to predict reduced surface brightness gradients for regions observed in face-on galaxies, and so they are unlikely to offer an explanation of our observations.

One of the most attractive aspects of our hypothesis is that it offers a promising scenario to account for the diffuse H α from gas dispersed over the disk of a galaxy outside the H II regions. Two quite recent studies have pointed to the emission of ionizing flux from OB stars as a satisfactory explanation of the H α emission from the warm ionized medium in disk galaxies. Oey & Kennicutt (1997) made a direct comparison of the rate of emission of ionizing photons from the OB stars in the Large Magellanic Cloud with the rate of H α emission from H II regions and concluded that up to 50% of the flux emitted by the stars is not down-converted within the H II regions and is thus available in principle to ionize the warm diffuse medium. They compare this with the estimate that 35% of the radiation is emitted by the diffuse medium in H α and conclude that the OB stars do put out sufficient flux in this galaxy. A study by

Ferguson et al. (1996) of NGC 247 and NGC 7793 concluded that the integrated flux required to ionize the diffuse gas is some 40% of the total H α flux emitted by a galaxy, including its H II regions. However, this calculation assumed, as have any such previous calculations, that the total flux of ionizing photons from an H II region can be directly measured using its H α flux. If the hypothesis presented in the present paper is correct, a significant fraction of the total ionizing flux liberated within the H II region population of a galaxy is not converted to Balmer radiation within the H II regions. This is true of the most luminous regions, with luminosities ranging up to 10^{40} ergs s^{-1} , and the escaping flux can range up to rather more than 10^{40} ergs s^{-1} for the brightest regions. The integrated escaping flux for a galaxy can attain a few times 10^{41} ergs s^{-1} , easily enough to account for the measured diffuse H α flux, according to the observations of Ferguson et al. (1996) and our own (Zurita et al. 2000). Ferguson et al. (1996) pointed out that the emitting diffuse gas tends to surround H II regions. We can go further on this point, noting the geometric correlation with the most luminous regions, which we will go further to quantify in a new study (Zurita et al. 2000). Finally, if our hypothesis is valid, a significant fraction of all the ionizing photons emitted by the OB stars in a galaxy may escape completely from the disk into the halo and finally into the intergalactic medium. Two corollaries are of interest here: (1) intergalactic clouds, even relatively far from a major galaxy, may have their surface layers ionized by this escaping flux (Bland, Hawthorne, & Maloney 1999) and (2) global star formation rates in disk galaxies, estimated from integrated H α fluxes, may in fact be significantly larger than these estimates. Both of these points are worth pursuing theoretically and observationally.

We should treat the density bounding-hypothesis for the luminous H II regions as speculative. Missing fundamental pieces of the puzzle are line-ratio tests of the sort performed by McCall, Rybski, & Shields (1985), comparing [O III] with [O II] emission-line intensities (in a density-bounded region, the [O II] Strömgren sphere should under many conditions be larger in radius than the H II region, so the [O III]/[O II] ratio should be significantly enhanced over its value in ionization-bounded regions). McCall et al. (1985) claimed one such detection, (region –606–1708) in NGC 598 and no others, but this detection has since been called into question (M. L. McCall 1999, private communication). Technical advances of the type represented by the TTF (Taurus tuneable filter; Bland-Hawthorn & Jones 1998), which permits imaging of complete galaxies in single emission lines with full redshift flexibility, will allow us to apply line-ratio tests to complete populations of fully imaged H II regions in galaxies such as the ones measured only in H α for the present paper. Another prospect, but only for the nearest galaxies because of limitations on angular resolution, is the use of two-dimensional fiber-fed spectrographs to sample the emission across the full face of an H II region. Here we would trade complete spectral coverage for a limitation on the number of H II regions. In both cases, we would hope to enhance understanding of the internal physics of the gas within the H II regions, measuring temperature and electron density as a function of position on a region and applying tests such as the [O III]/[O II] emission ratio to the question of density bounding.

The apparent invariance in the luminosity of the glitch measured in the LF does offer a possible refined secondary

standard candle of high luminosity and constant presence for use well into the Hubble flow, regardless of whether the interpretation we have placed on it in the present article is fully or even partially valid. To demonstrate its scope will require amplification of the number of objects studied to determine reliably, using local galaxies, the scatter in the observed feature, including any possible dependence on galaxy luminosity and type, and to calibrate it using galaxies whose Cepheid distances have been determined in the *HST* Key Project.

The William Herschel Telescope is operated on the island of La Palma by the Royal Greenwich Observatory in the

Spanish Observatorio del Roque de los Muchachos of the Instituto de Astrofísica de Canarias. This work was partially supported by the Spanish DGICYT (Dirección General de Investigación Científica y Técnica) by grants PB91-0525 and PB94-1107. This research has made use of the NASA/IPAC Extragalactic Database, which is operated by the Jet Propulsion Laboratory, California Institute of Technology, under contract with the National Aeronautics and Space Administration. Thanks are due to Andrew Cardwell for a series of computational tests related to the H II region luminosity function. We are grateful to Chris McKee and to the referee, Marshall McCall, for comments that have helped improve this paper.

REFERENCES

- Aaronson, M., & Mould, J. 1986, *ApJ*, 303, 1
 Arsenault, R., Roy, J. R., & Boulesteix, J. 1990, *A&A*, 234, 23
 Bland-Hawthorn, J., & Jones, D. H. 1998, *Publ. Astron. Soc. Australia*, 44
 Bland-Hawthorne, J., & Maloney, P. R. 1999, *ApJL*, 510, L33
 Cepa, J., & Beckman, J. E. 1989, *A&AS*, 79, 41
 ———. 1990, *A&AS*, 83, 211
 Dove, J. B., & Shull, J. M. 1994, *ApJ*, 430, 222
 Elmegreen, B. G. 1997, *ApJ*, 486, 944
 Ferguson, A. M., Wyse, R. G., Gallagher, J. S., & Hunter, D. A. 1996, *AJ*, 111, 2265
 García Vargas, M. L., Bresan A., & Diaz A. I. 1995, *A&AS*, 112, 13
 Heiles, C. 1990, *ApJ*, 354, 483
 Hodge, P. W. 1987, *PASP*, 99, 915
 Hummer, D. G., & Seaton, M. J. 1964, *MNRAS*, 127, 217
 Kennicutt, R. C. 1984, *ApJ*, 287, 116
 Kennicutt, R. C., Edgar, B. K., & Hodge, P. W. 1989, *ApJ*, 337, 761
 Kingsburgh, R. W., & McCall, M. L. 1998, *AJ*, 116, 2246
 Knapen, J. H. 1998, *MNRAS*, 297, 255
 Knapen, J. H., Arnth-Jensen, N., Cepa, J., & Beckman, J. E. 1993, *AJ*, 106, 56
 Larson, R. B. 1982, *MNRAS*, 200, 159
 Massey, P., & Hunter, D. A. 1998, *ApJ*, 493, 180
 Massey, P., Johnson, K. E., & DeGioia-Eastwood, K. 1995a, *ApJ*, 454, 151
 Massey, P., Lang, G. C., DeGioia-Eastwood, K., & Garmany, C. D. 1995b, *ApJ*, 438, 188
 McCall, M. L., Rybski, P. M., & Shields, G. A. 1985, *ApJS*, 57, 1
 McCall, M. L., Straker, R. W., & Uomoto, A. K. 1996, *AJ*, 112, 1096
 McKee, C. F., & Williams, J. P. 1997, *ApJ*, 476, 144 (MW)
 Norman, C. A., & Ikeuchi, S. 1989, *ApJ*, 345, 372
 Oey, M. S., & Kennicutt, R. C. 1997, *MNRAS*, 289, 827
 Osterbrock, D. E. 1989, *Astrophysics of Gaseous Nebulae and Active Galactic Nuclei* (Mill Valley: University Science Books)
 Pleuss, P., & Heller, C. H. 2000, *A&A*, submitted
 Rand, R. J. 1992, *AJ*, 103, 815
 Rozas, M., Beckman, J. E., & Knapen, J. H. 1996a, *A&A*, 307, 735
 Rozas, M., Castañeda, H. O., & Beckman, J. E. 1998a, *A&A*, 330, 873
 Rozas, M., Knapen, J. H., & Beckman, J. E. 1996b, *A&A*, 312, 275
 Rozas, M., Sabalisk, N. S., & Beckman, J. E. 1998b, *A&A*, 338, 15
 Rozas, M., Zurita, A., & Beckman, J. E. 2000, *A&A*, 354, 823
 Rozas, M., Zurita, A., Heller, C. H., & Beckman, J. E. 1999, *A&AS*, 135, 145
 Sabalisk, N. S., Tenorio-Tagle, G., Castañeda, H. O., & Muñoz-Tuñon, C. 1995, *ApJ*, 444, 200
 Salpeter, E. 1955, *ApJ*, 121, 161
 Sciama, D. W. 1990, *ApJ*, 364, 549
 Strömgren, B. 1939, *ApJ*, 89, 526
 Tenorio-Tagle, G., Muñoz-Tuñón, C., & Cox, P. D. 1993, *ApJ*, 418, 767
 Terlevich, R., & Melnick, J. 1981, *MNRAS*, 195, 839
 Tully, R. B. 1987, *Nearby Galaxies Catalog* (New York: Cornell Univ. Press)
 Vacca, W. D., Garmany, C. D., & Shull, M. J. 1996, *ApJ*, 460, 914
 Walterbos, R. A. M., & Braun, R. 1992, *A&AS*, 92, 625
 Zanstra, H. 1931, *Z. Astrophys.*, 2, 1
 Zurita, A., Rozas, M., & Beckman, J. E. 2000, *A&A*, submitted